Materials and Design 47 (2013) 323–330

Contents lists available at SciVerse ScienceDirect

Materials and Design

journal homepage: www.elsevier.com/locate/matdes

Technical Report

Tensile and fracture toughness of high strength β Titanium alloy, Ti–10V–2Fe–3Al, as a function of rolling and solution treatment temperatures

G. Srinivasu [a], Y. Natraj [b], A. Bhattacharjee [c,*], T.K. Nandy [c], G.V.S. Nageswara Rao [a]

[a] NIT Warangal, Met. & Matls. Engg., Warangal 506004, AP, India
[b] IIT Kharagpur, Met. & Matls. Engg., Kharagpur 721302, WB, India
[c] DMRL, P.O. Kanchanbagh, Hyderabad 500058, AP, India

ARTICLE INFO

Article history:
Received 24 March 2012
Accepted 28 November 2012
Available online 8 December 2012

ABSTRACT

The effect of processing and heat treatment has been studied on tensile properties and fracture toughness of a high strength metastable beta titanium alloy, Ti–10V–2Fe–3Al. The alloy was double melted by vacuum arc melting and subsequently subjected to thermomechanical processing that included combinations of rolling and solution heat treatment both in α–β and β phase fields. Rolling temperatures were varied from 710 °C (sub-transus) to 860 °C (super-transus) and solution treatment temperatures were varied from 710 °C (sub-transus) to 830 °C (super-transus). A systematic microstructural investigation (optical as well as scanning electron microscopy) was undertaken in order to correlate the property trends with underlying microstructure which is strongly dependent on the thermomechanical processing sequence. A subtransus rolling followed by subtransus solution treatment resulted in equiaxed α morphology whereas a supertransus rolling followed by subtransus solution treatment resulted in more acicular/lenticular morphology of α phase. While α–β rolling followed by α–β heat treatment gave better tensile properties, β rolling followed by α–β heat treatment resulted in superior fracture toughness.

1. Introduction

Beta titanium alloys form one of the most versatile classes of materials with respect to processing, microstructure and mechanical properties [1,2]. They offer an attractive alternative to α/β alloys due to their increased heat treatability, wide and unique range of strength-to weight ratios, deep hardening potential and inherent ductility. On density-normalized basis they can surpass maraging steels in appropriate heat treatment condition. In recent times, beta titanium alloys have been inducted in airframe applications because of their high strength and damage tolerance properties [3]. Today, beta titanium alloys possess a reasonable share of market for aerospace applications (Fig. 1). Amongst beta titanium alloys Ti–15Al–3Cr–3Al–3Sn (Ti-15-3-3-3) and Ti–10V–2Fe–3Al (Ti-10-2-3) have been used for a variety of airframe applications [3,4].

The alloy Ti–10V–2Fe–3Al was developed by Timet in 1970. It has capability to replace precipitation-hardening steels because of its deep hardenability and good ductility. It received a major breakthrough in aerospace applications when it was used as landing gear in Boeing 777 [2,4]. While the initial cost of the alloy was higher than 4340 steel that was used for the landing gear applications, the cost benefit for using the alloy was realised in long run since components made out of steel needed to be replaced over one lifetime of the aircraft because of its susceptibility to stress corrosion cracking. Additionally replacement of steels by Ti-10-2-3 resulted in weight saving of 270 kg per aircraft. C-17, a McDonnell Douglas military transport aircraft also uses Ti-10-2-3 alloy for landing gear applications. The alloy is used in numerous other airframe applications such as wings, fuselage, doors, nacelles and cargo handling structures. Another potential application for the alloy Ti-10-2-3 is slat/flap tracks that can be fabricated using alloy forgings [4,5]. Slats/flap increases the effective wing area; enhances lift and drag during take-off and landing respectively. Tracks are the moving beams enabling load transmission and movement between wings and moving slats. They are generally made of maraging steel. However, in the recent past, flap tracks that are fitted on the trailing side of the wings for performing similar functions have been made of Ti-10-2-3. By using six 5 ft. long flap tracks in Boeing 777, the total weight saving was about 40 kg [5]. The alloy Ti-10-2-3 has been in use for quite some time and although new alloys such as (Ti–5A–5Mo–5V–3Cr (Ti5553)) have been developed for larger size forgings because of deeper hardenability [4], Ti-10-2-3 still holds its advantageous position for medium size forgings up to about 60–75 mm thick [3].

Interrelationship between processing and microstructure of Ti-10-2-3 have been studied by several researchers in past. Hall [6] has discussed the effect of forging variables on the microstructure of Ti-10-2-3. A comprehensive and detailed review of

* Corresponding author. Tel.: +91 40 24586601; fax: +91 40 24342123.
E-mail address: amitb@dmrl.drdo.in (A. Bhattacharjee).

0261-3069/$ - see front matter © 2012 Elsevier Ltd. All rights reserved.
http://dx.doi.org/10.1016/j.matdes.2012.11.053

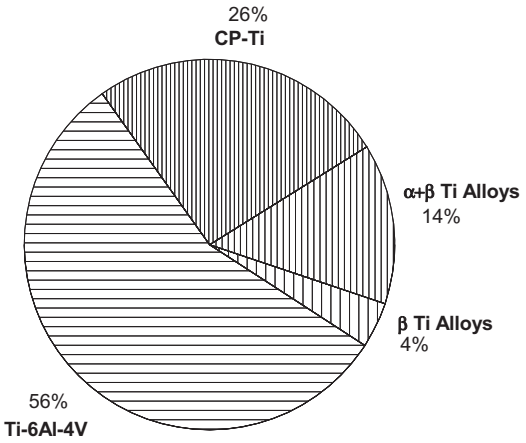

Fig. 1. Market share of different alloys for US aerospace applications [30].

thermomechanical processing of β titanium alloys has been carried out by Weiss and Semiatin [7]. Robertson and McShane [8] have studied isothermal hot deformation behaviour of Ti-10-2-3.

In addition, there have been numerous studies relating microstructure and mechanical properties. Terlinde et al. [9] have studied the effect of microstructure on tensile deformation and fracture of Ti-10-2-3, whereas Duerig et al. [10] had reported the effect of microstructure of the alloy on fatigue crack propagation. Jha and Ravichandran [11] have evaluated the effect of mean stress (stress ratio) and ageing on fatigue crack growth. Optimization of low cycle fatigue, fatigue crack propagation resistance and fracture toughness has been carried out by Kuhlman et al. [12] through microstructural modification. The LCF behaviour of Ti-10-2-3 has been studied by Luquiau et al. [13]. Kuhlman and Chakrabarti [14] have also investigated the effect of microstructure on fatigue and fatigue crack growth rate of titanium alloy. The effect of β fleck on the properties of Ti-10-2-3 has been examined by Zhou et al. [15]. Jiaxuan and Zhongquan [16] have established relationship between mechanical properties, microstructure and processing parameters of the alloy, but studies that correlate thermo-mechanical processing of Ti-10-2-3 with microstructure, tensile and fracture toughness are scarce. Fracture toughness assumes a considerable significance in the selection of materials for modern day aircrafts which are designed based on damage tolerance. In the present investigation, a systematic attempt has been made to correlate rolling and heat treatment of the alloy with microstructure and mechanical properties. Different microstructures have been generated as a function of rolling and solution treatment temperature. This is followed by evaluation of tensile and fracture toughness. Subsequently, interrelationships between rolling and solution treatment temperature, microstructures and mechanical properties have been attempted.

2. Experimental details

The alloy was melted using double vacuum consumable arc melting process to obtain an ingot of 110 mm length and 145 mm diameter. This was followed by machining and radiography in order to remove defective portions from top and bottom of the ingot. Forging was carried out at 925 °C using 100 Ton pneumatic hammer forge to obtain 30 mm thick slab that was subsequently rolled to 15 mm thick plate using a 200 Ton two high mill at different temperatures. Four different rolling temperatures (RT) were chosen based on β transus temperature, determined employing heat treatment at different temperatures followed by metallography. Blanks were cut from rolled plates and subjected to α−β and β solution treatments (STs) (Table 1) followed by a common ageing treatment of 500 °C/4 h/air-cool.

Table 1
Shape of prior β grains as a function of rolling and solution treatment temperatures.

Solution treatment temperature (°C)	Rolling temperature (°C)	Shape of prior β grains
710	710	Elongated
	760	Elongated
	810	Equiaxed
	860	Equiaxed
760	710	Elongated
	760	Elongated
	810	Equiaxed
	860	Equiaxed
830	710	Partially elongated
	760	Partially elongated
	810	Equiaxed
	860	Equiaxed

Specimens for optical and scanning electron microscopy were prepared using standard metallography polishing technique. Subsequently for optical microscopic investigation, the specimens were etched using Kroll's reagent [17], while for SEM study, the specimens were used in as polished condition. While Leitz optical microscope was used for the examination of microstructure, FEI make ESEM at an operating voltage of 20 kV was used for the examination of microstructure and fractographs. Back scatter electron (BSE) mode was used for recording microstructures and secondary electron mode was used for studying fractographs.

The heat treated blanks were machined to obtain standard tensile specimens (4 mm nominal dia. × 25 mm gauge length). The testing was carried out in a 100 kN screw driven Instron 5500R with a cross speed of 1 mm/min corresponding to an approximate strain rate of 10^{-3}/s 35 × 32 × 15 mm^3 specimens (1/2 TCT in long transverse (LT) orientation as per *ASTM E399-09e2*) were machined for fracture toughness evaluation. Initially, the specimens were fatigue pre-cracked at a constant load ratio *R*, defined as the ratio between the minimum and the maximum load, which was maintained constant at 0.1. In all the cases, the notch was machined to a depth of around 0.4 times the width of the specimen (*W*) and fatigue crack was grown up to 0.55–0.6 W. Fatigue precracking was carried out as per the procedure described in ASTM: E647-11e1. Fracture toughness tests were carried out in a servo-hydraulic digital control Instron 8500 plus test system. During the test 5 mm gauge length with 2 mm extension clip COD gauge was used to record crack opening displacement.

3. Results

Optical microstructures of 710 °C and 830 °C solution treated (ST) plus aged specimens for two different rolling temperatures (710 and 860 °C) are shown in Fig. 2. The 710 °C rolling followed by 710 °C ST yields an elongated or pancake prior β structure, whereas rolling at 860 °C followed by solution treatment at 830 °C shows a equiaxed prior β structure. Table 1 summarises optical microstructure for different combinations of rolling and solution treatment conditions.

BSE SEM microstructures show the distribution and morphology of primary α for different combinations of rolling and ST temperatures (Figs. 3–5). Fig. 3 shows micrographs of specimens rolled at different temperatures (710–860 °C) followed by a ST at 710 °C and ageing (500 °C/4 h/AC). The specimens rolled in α−β temperature region viz. 710 °C (Fig. 3a) and 760 °C (Fig. 3b), show equiaxed plus elongated α in aged β matrix that is unresolved at SEM level. The 760 °C rolled specimen shows lower volume fraction of pri-

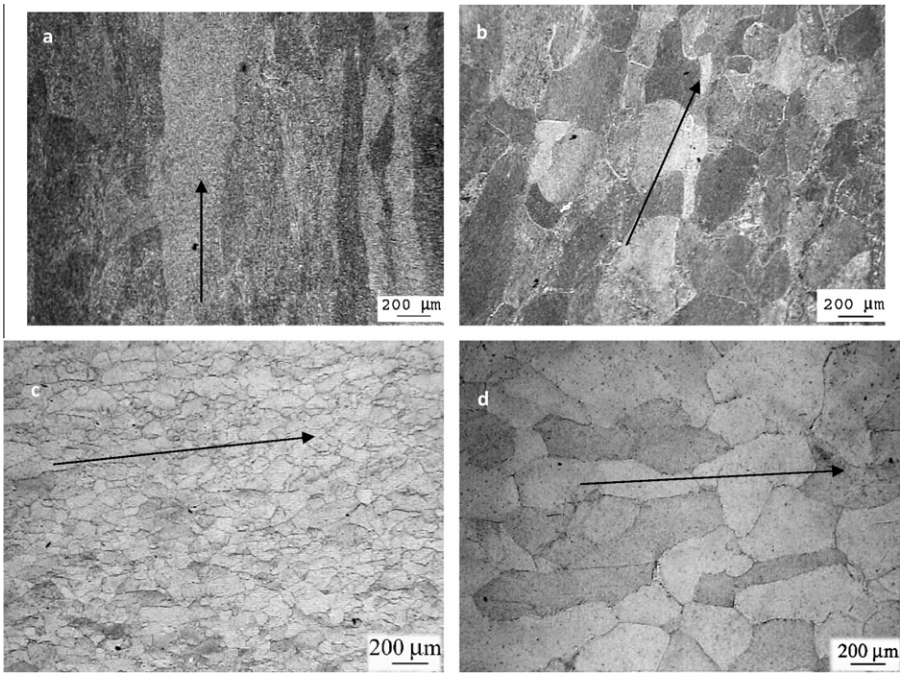

Fig. 2. Optical microstructures showing morphology of prior β grains as a function rolling temperatures at constant solution treatment temperatures. For rolling temperatures of (a) 710 °C (sub transus) and (b) 860 °C (super transus) and solution treatment at 710 °C (sub transus). For rolling temperatures of (c) 710 °C (sub transus) and (d) 860 °C (super transus) and solution treatment at 830 °C (super transus). The arrows indicate the rolling direction.

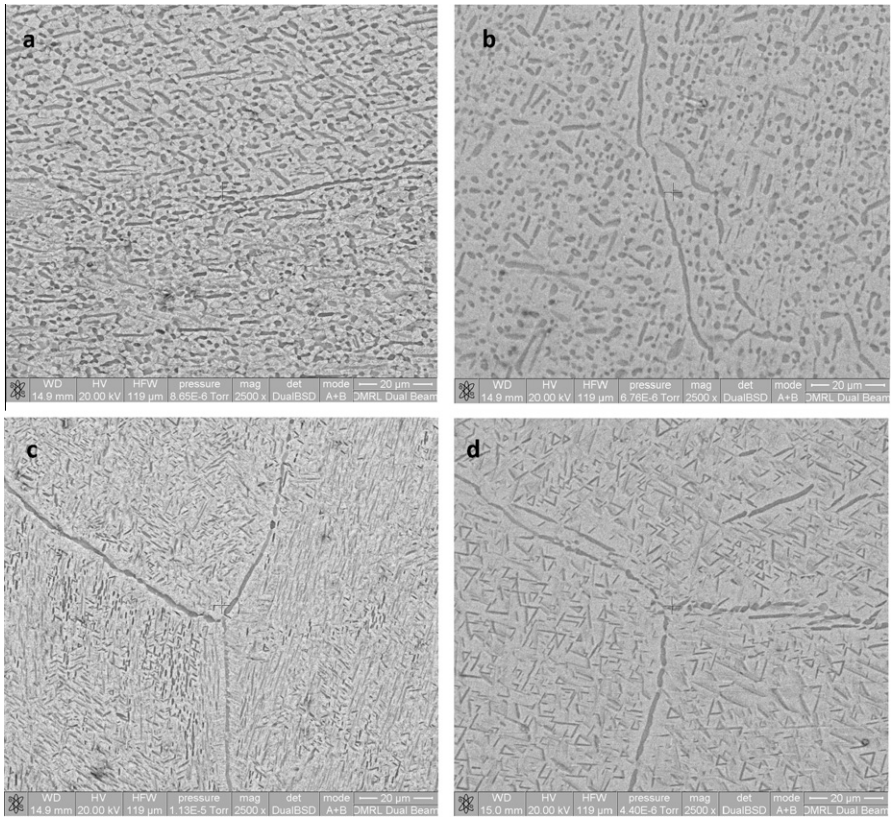

Fig. 3. Microstructural evolution of Ti–10V–2Fe–3Al as a function of rolling temperature at a fixed solution treatment temperature of 710 °C. The rolling temperatures were (a) 710 °C (b) 760 °C (c) 810 °C and (d) 860 °C.

mary α as compared to 710 °C rolled specimen. Specimens rolled above β transus, at 810 °C (Fig. 3c) and 860 °C (Fig. 3d) show lenticular α. Presence of continuous grain boundary α is seen in 760, 810 and 860 °C rolled specimens (Fig. 3b–d). Similar microstructures are seen in 760 °C ST specimens (Fig. 4a–d), the difference being lower volume fraction of primary α especially equiaxed α (Fig. 4a and b). Again continuous grain boundary α is seen in 760, 810 and 860 °C rolled specimens. Microstructures of specimens solu-

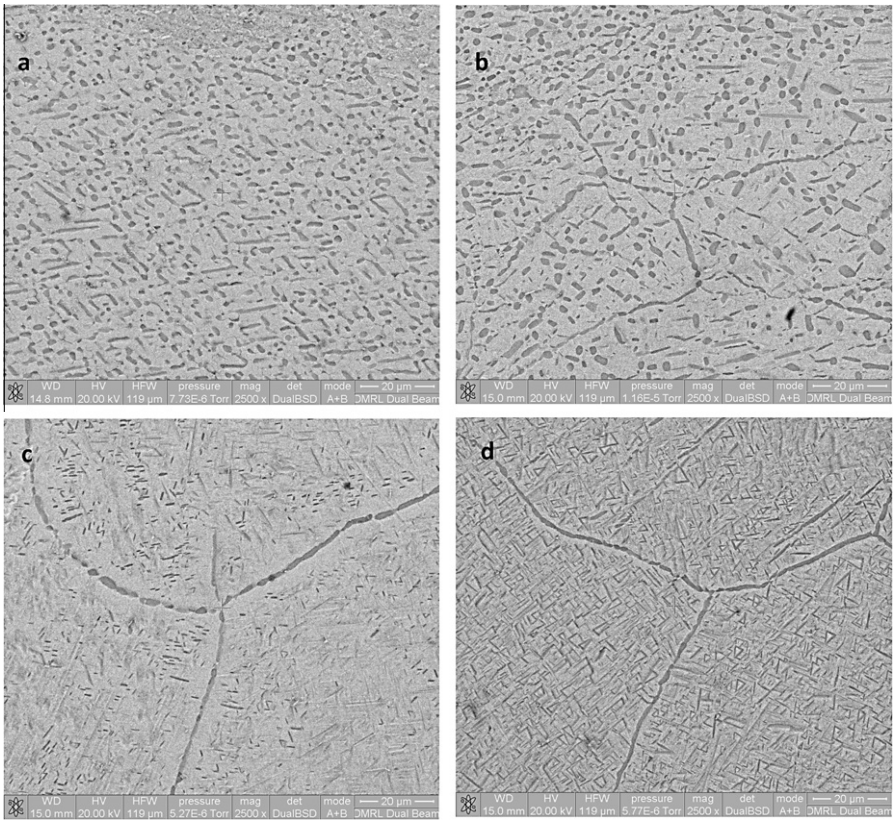

Fig. 4. Microstructural evolution of Ti–10V–2Fe–3Al as a function of rolling temperature at a fixed solution treatment temperature of 760 °C. The rolling temperatures were (a) 710 °C (b) 760 °C (c) 810 °C and (d) 860 °C.

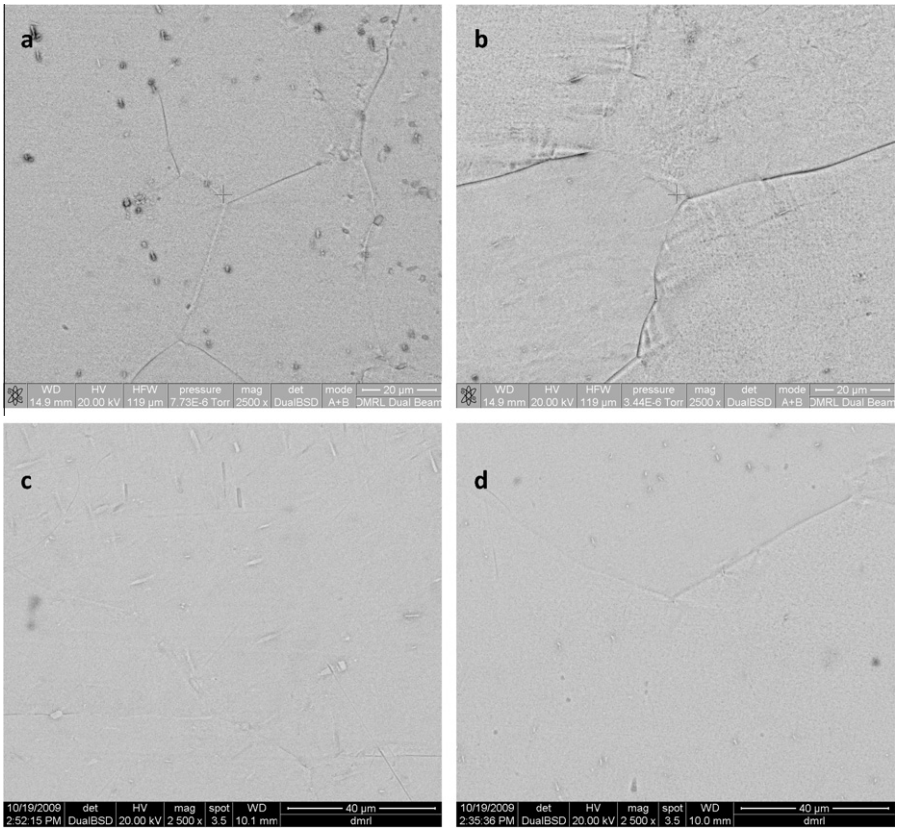

Fig. 5. Microstructural evolution of Ti–10V–2Fe–3Al as a function of rolling temperature at a fixed solution treatment temperature of 830 °C. The rolling temperatures were (a) 710 °C (b) 760 °C (c) 810 °C and (d) 860 °C.

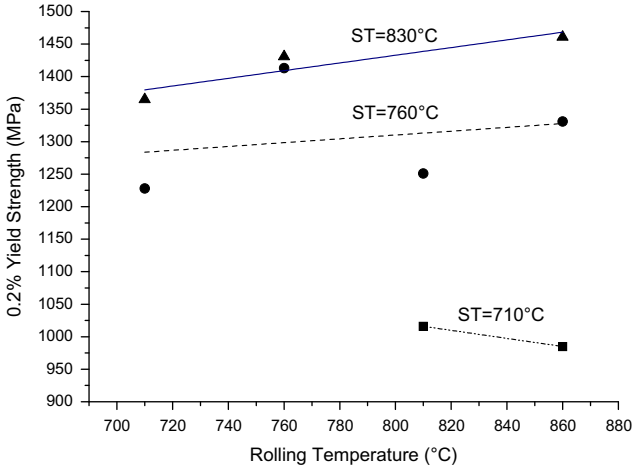

Fig. 6. 0.2% Yield strength of the alloy as a function of rolling temperature at different solution treatment temperatures. The alloy was given a common ageing treatment of 500 °C/4 h/AC.

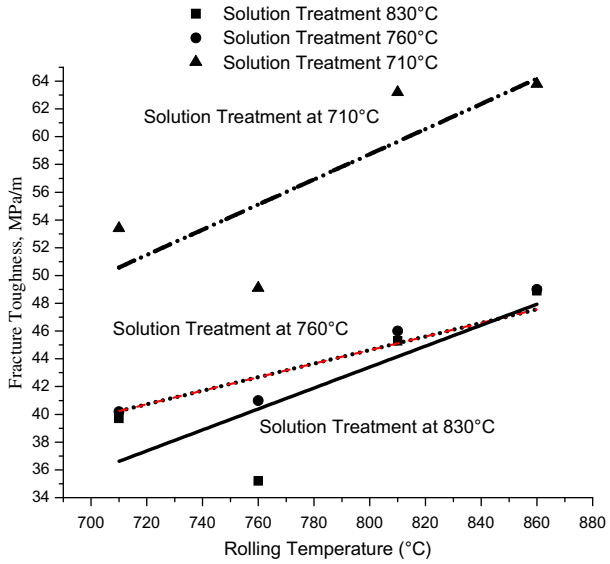

Fig. 7. Effect of varying processing conditions (viz rolling temperature at constant solution treatment temperatures) on fracture toughness of Ti–10V–2Fe–3Al.

Table 2
Fracture toughness (K_{1G}, MPa$\sqrt{m}$) of Ti–10V–2Fe–3Al as a function of rolling and solution treatment temperature for a constant ageing treatment of 500 °C/4 h/AC.

Solution treatment temperature (°C)	Rolling temperature (°C)			
	710	760	810	860
710	53.4	49.1	63.2	63.8
760	40.2	41.0	46.0	49.0
830	39.7	35.2	45.3	48.9

tion treated at 830 °C are shown in Fig. 5. In all cases, a fine microstructure (unresolved at 1000–5000× magnification) is observed. Coarsening of β grain size is apparent with increasing RT.

Fig. 6 shows the variation of yield strength of the alloy as a function of RT at constant ST temperatures. The yield strength changes gradually with RT, increases in case of 760 °C and 830 °C ST and decreases for 710 °C ST. The ST temperature has a profound influence on the yield strength of the alloy as the strength values increase with increasing ST temperature at a constant RT. Fracture toughness values for different combination of ST and RT are shown in Table 2. Fig. 7 shows fracture toughness vs. RT plot for different ST temperature. For a constant ST temperature, the fracture toughness increases with increasing RT. Fig. 8 is a replot of Fig. 7 showing fracture toughness as a function of solution treatment temperature at constant rolling temperatures. As the ST temperature increases, fracture toughness decreases. Highest fracture toughness values are obtained for super transus rolling (810 and 860 °C), and low α–β ST temperature (710 °C). On the other hand, higher ductility values are obtained for a subtransus rolling followed by a sub-transus ST (Table 3).

4. Discussion

The initial processing of the as melted ingot of titanium alloys is carried out in β phase field at temperatures ranging from $T_\beta + 100$ °C to $T_\beta + 200$ °C. The primary objectives of β processing are to breakdown the cast dendritic structure and to homogenize the alloy by eliminating the inter-dendritic micro-segregation. This is followed by deformation in α–β region (soaking temperature of $T_\beta - 50$–$T_\beta - 100$ °C). Controlled amount of deformation (10–20%) is imparted in α–β region in order to obtain optimal size, shape and volume fraction of α. Deformation in α–β region leads to

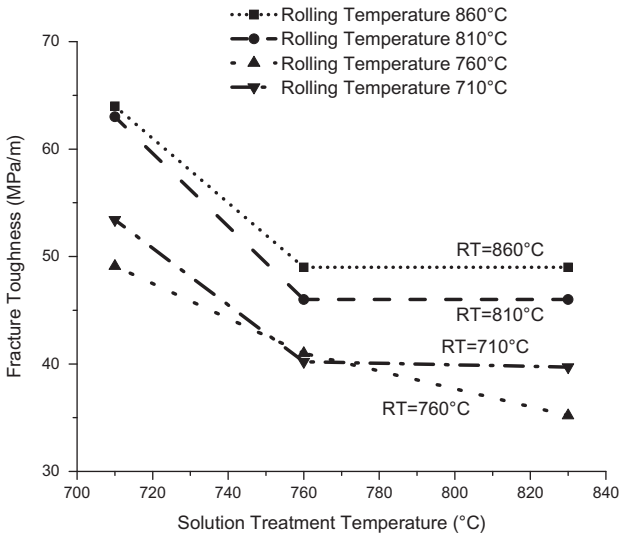

Fig. 8. Effect of varying processing conditions (viz solution treatment temperature at constant rolling temperatures) on fracture toughness of Ti–10V–2Fe–3Al.

Table 3
Tensile properties of Ti–10V–2Fe–3Al as a function of rolling and solution treatment temperature.

S. no.	Solution treatment temperature (°C)	Rolling temperature (°C)	Yield stress (MPa)	%El
1	830	860	1461	0.5
2	830	760	1431	1.0
3	830	710	1365	0.7
4	760	860	1331	2.4
5	760	760	1413	2.7
6	760	710	1228	6.0
7	710	710	1120	10.2

breaking up of grain boundary α and reduction in aspect ratio of α particles resulting in optimum balance of strength, ductility and fracture toughness [18]. In the present study, both rolling

and solution treatment temperatures were varied in order to generate a range of microstructures and then its effect on tensile and fracture toughness were studied.

Three microstructural parameters namely prior β grain size and shape, morphology of primary α and fine structure of aged β (type I/type II α and retained β) are of key importance and known to have considerable influence on properties of β titanium alloys [19–21]. As seen in Table 1 and Fig. 2, shape of β grains is significantly influenced by thermomechanical processing. For rolling in α–β region (710 and 760 °C), equiaxed β grains are obtained for ST near β or above β transus, whereas α–β ST results in pancake type of structure pointing towards un-recrystallised β grains. Similarly for 830 °C (above β transus) rolling, equiaxed β structures are obtained in β ST condition only. This is in contrast to near α and α–β titanium alloys where recrystallisation of both α and β is realised by processing and heat treatment of the alloy in α–β region (T_β - 50 to T_β - 100 °C [22]). The reason for this is twofold: (1) the processing temperatures (700–850 °C) are considerably lower (as opposed to 950–1000 °C, in near α and α–β titanium alloys) resulting in considerably reduced diffusion kinetics and delaying the recrystallisation process [23] and (2) presence of α during α–β processing further retards recrystallisation by pining prior β boundaries. Therefore recrystallisation of β is obtained only at higher solution treatment temperature that not only provides a greater driving force for recrystallisation but also lower volume fraction of α.

Equiaxed morphology of α is obtained by α–β processing and α–β ST. The results are consistent with the work done by Bhattacharjee et al. [24] who have clearly shown that recrystallised α structure is obtained in metastable β alloys by processing them at T_β - 50 to T_β - 100 °C. Margolin and Cohen [25,26] proposed a model for the globularisation of both the lamellar α plates within the prior beta grains as well as grain boundary α. The mechanism by which the process proceeds is shown in Fig. 9. Initially, the recrystallised α grains are formed within the α plate (Fig. 9b). Surface tension requirements do not permit a 180° dihedral angle to exist between the α/α boundary and the β plate boundary. Thus a driving force is provided for the movement of some beta phase into the α/β boundaries and a simultaneous rotation of the of the α/β boundaries toward one another (Fig. 9c). Such a rotation enlarges the recrystallised α grain to a size larger than the original plate thickness bringing it into contact with the adjacent α plate, which may or may not have recrystallised. Subsequent working separates the neighbouring α plates. Fig. 10a shows ingress of β phase in neighbouring α phase.

Yield strength increases with increasing RT for both α–β (760 °C) and β (830 °C) ST (Fig. 6). In the α–β ST condition, increasing RT will result in decreasing volume fraction of soft equiaxed α (Fig. 10) and increasing volume fraction of lenticular α. Increase in strength is a result of increasing volume fraction of lenticular α which is expected to shear during deformation because of the orientation relationship with parent β and thereby provide shear strengthening. Increasing RT for 760 °C ST also results in decreasing ductility (Table 3). The 830 °C ST, RT was expected to play an insignificant role on strength and ductility. Yet, an increase in strength is observed. Reason for this is not clear, although a study of texture, which is expected to be dependent on the processing condition, may be needed to understand this issue.

Fig. 6 also shows that at constant RT, increasing ST temperature leads to increase in yield strength. This is attributed to decrease in volume fraction of soft primary α (equixaed or lenticular) and increase in aged β which is stronger. It is also seen that lower rolling and ST temperature results in higher ductility (Table 3). This can be ascribed to the formation of soft equiaxed α. The volume fraction of equiaxed α decreases with increase in rolling and ST temperature.

Fracture toughness is primarily governed by three microstructural components: (i) morphology of α (ii) volume fraction of aged β and (iii) presence/absence of continuous/discontinuous grain boundary α. Lenticular α has been shown to improve the fracture

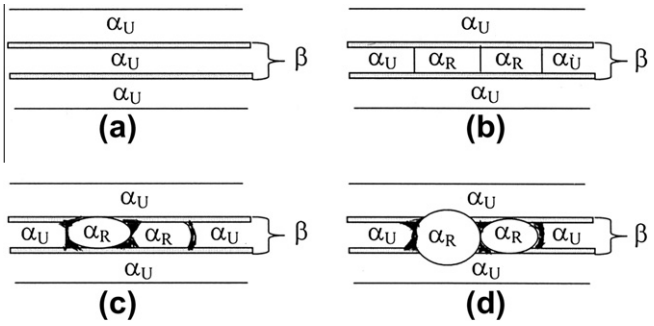

Fig. 9. Schematic illustration of the mechanism of globularisation of Widmanstatten α in α/β titanium alloys. (a) Unrecrystalliased α and β. (b) Beginning of recrystallisation. (c) α_R moving into Widmanstatten α side plates. (d) α_R consuming widmanstatten α side plates. α_U = unrecrystallised α; α_R = recrystaliised α; β = beta [25,26].

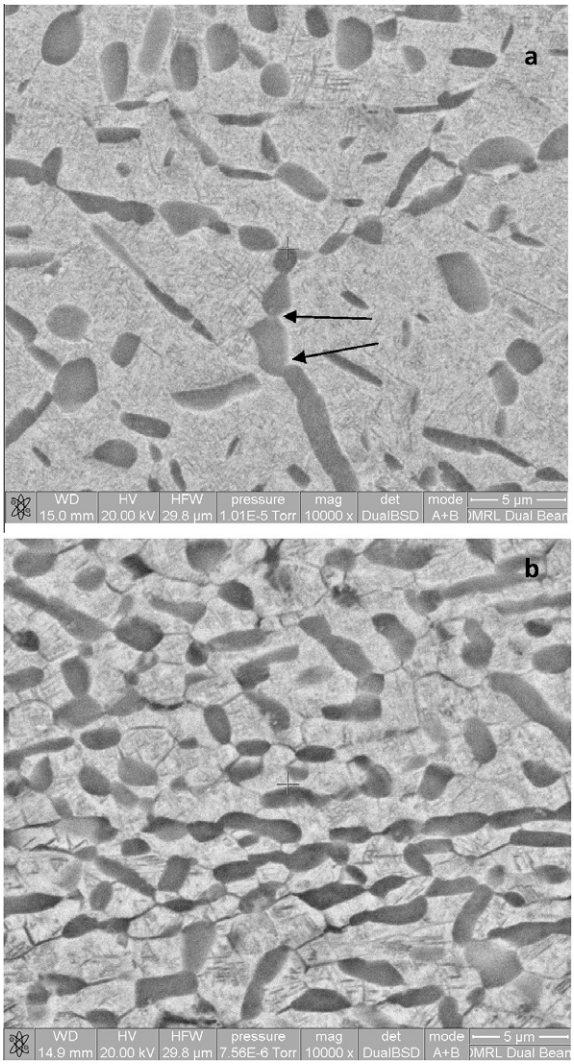

Fig. 10. Ti–10V–2Fe–3Al rolled at 710 °C, but solution treated at (a) 760 °C and (b) 710 °C and aged at 500 °C/4 h/AC. Higher volume fraction of equiaxed primary α is clearly seen in (b). The arrows indicate the phenomena of pinching of α grains in progress due to ingress of β phase ultimately leading to globalisation of α phase as explained in the model by Margolin and Cohen [25,26] occurring in the alloy.

toughness by increasing the tortuosity of the crack path [19,1,27–29]. For the same volume fraction, presence of equiaxed α results in lower fracture toughness as the fracture path is relatively straighter resulting in considerably less energy absorption. Aged β that is a fine aggregate of α and retained β is inherently less ductile and significantly stronger. This leads to smaller plastic zone size ahead of the crack tip leading to lower fracture toughness. Presence of continuous grain boundary α surrounded by a softer precipitate free zone leads to flow localisation, thereby influencing fracture toughness values adversely. The fracture toughness trends with respect to rolling and ST temperature can be explained with the help of microstructural features discussed above. Increase in fracture toughness with increasing RT can be explained as follows. For a ST temperature of 710 °C, lower RT (710 °C and 760 °C) yields equiaxed α microstructure that is associated with lower fracture toughness. On the other hand, for the same ST temperature, rolling at or above β transus (810 and 860 °C) results in the formation of lenticular α thereby yielding higher fracture toughness values. A similar trend is discernable for 830 °C ST condition in which case the microstructure consists of aged β with grain boundary α. This is in agreement with strength values which increase with increasing RT. Finally, decreasing fracture toughness with increasing ST temperature (Fig. 7) is attributed to increasing volume fraction of aged β that is relatively more brittle and stronger as compared to primary α.

5. Conclusions

The effect of processing and heat treatment has been studied on tensile properties and fracture toughness of a high strength metastable beta titanium alloy, Ti–10V–2F3e–3Al. The following conclusions can be drawn from the study.

(1) A lower subtransus rolling followed by a subtransus solution treatment (+ageing) of Ti-10-2-3 alloy leads to the formation of equiaxed primary α phase, whereas, supertransus rolling followed by a substransus solution treatment (+ageing) leads to a more acicular/lenticular α phase morphology.
(2) Supertransus solution treatment followed by ageing results in the fine aged β microstructure regardless of the processing temperature.
(3) A supertransus solution treatment (regardless of processing temperature) results in higher strength and lower ductility, while a subtransus solution treatment following a subtransus rolling leads to a lower strength but higher ductility.
(4) A subtransus (about $T_\beta - 90$ °C) solution treatment plus ageing following supertransus rolling results in higher fracture toughness.
(5) While equiaxed alpha structure promotes tensile ductility, high fracture toughness is obtained in lenticular alpha microstructure.

Acknowledgements

The authors are grateful to Director DMRL for his constant encouragement throughout the course of this work and also for allowing to publish this work. The authors would like to thank the members of the Titanium Alloy Group, for their experimental support. The members of the Mechanical Engineering and Mechanical Behaviour groups are also gratefully acknowledged for the fabrication and testing of the numerous tensile and fracture toughness specimens used in this study. One of the authors, Dr. G.V.S. Nageswara Rao would also like to thank the ARDB board, since the work was possible due to the grant received under ARDB Project No. DARO/08/1444/M/I.

References

[1] Terlinde G, Fischer G. Beta titanium alloys. In: Blenkinsop PA, Evans WJ, Flower HM, editors. Titanium '95. Science and technology; 1996. p. 2177–93.
[2] Boyer RR. Aerospace applications of beta titanium alloys. J Metal 1994;46(7):20–3.
[3] Boyer RR. Attributes, characteristics and application of titanium and its alloys. J Met May 2010;62(5):21–6.
[4] Boyer RR, Briggs RD. The use of β titanium alloys in the aerospace industry. J Mater Eng Perform 2005;14(6):681–5.
[5] Boyer RR. Applications of beta titanium alloys in airframes. In: Eylon D, Boyer RR, Koss DA, editors. Beta titanium alloys in the 1990's. Pennsylvania (Warrendale): TMS; 1993. p. 335–46.
[6] Hall IW. Effect of forging variables on the microstructure of Ti–10V–2Fe–3Al. In: Lutjering G, Zwicker U, Bunk W, editors. Ti: science and technology, the proceedings of the Vth international conference in Ti, vol. I. Munich (Germany);1984. p. 491–8.
[7] Weiss I, Semiatin SL. Thermo-mechanical processing of beta titanium alloys – an overview. Mater Sci Eng 1998;A 243:46–65.
[8] Robertson DG, McShane HB. Isothermal hot deformation behavior of metastable β titanium alloy, Ti–10V–2Fe–3Al. Mater Sci Technol 1997;13(July):575–83.
[9] Terlinde GT, Duerig TW, Williams JC. Microstructure, tensile deformation and fracture in aged Ti–10V–2Fe–3Al. Met Trans Oct 1983;14A:2101–15.
[10] Duerig TW, Allison JE, Williams JC. Microstructural influences on fatigue crack propagation in Ti–10V–2Fe–3Al. Met Trans 1985;16A:739–51.
[11] Jha SK, Ravichandran KS. Effect of mean stress (stress ratio) and ageing on fatigue crack growth in a metastable beta titanium alloy, Ti–10V–2Fe–3Al. Met Trans 2000;31A(March):703–14.
[12] Kuhlman GW, Chakrabarti AK, Yu TL, Pishko R, Terlinde IW. LCF, fracture toughness and fatigue crack propagation resistance optimisation in Ti–10V–2Fe–3Al through microstructural modification. In: Chakrabarti AK, Chestnut JC, editors. Proceedings of the annual symposia on 'Effect of microstructure fatigue and fatigue crack growth rate on titanium alloys', held in Denver Colorado. Warandale (Penn): TMS-AIME; 1987. p. 171–91.
[13] Luquiau D, Feaugas X, Campagnac MH, Clavel M. Low cycle fatigue behavior of Ti–10V–2Fe–3Al. In: Blenkinsop PA, Evans WJ, Flower HM, editors. Titanium 95, science and technology. London: Institute of Materials; 1996. p. 1147–55.
[14] Kuhlman GW, Chakrabarti AK. Room temperature fatigue crack propagation in beta titanium alloy. In: Chakrabarti AK, Chestnut JC, editors. Proceedings of the annual symposia on 'effect of microstructure fatigue and fatigue crack growth rate on titanium alloys', held in Denver Colorado. Warandale (Penn): TMS-AIME; 1987. p. 3–16.
[15] Zhou YG, Tang JL, Yu HQ, Zeng WD. On Effect of beta fleck on properties of Ti–10V–2Fe–3Al. In: Froes FH, Caplan I, editors. Titanium 1992, science and technology. The Minerals, Metals and Materials Society; 1993. p. 513–22.
[16] Jiaxuan W, Zhongquan D. Relationship between mechanical properties, microstructure and processing parameters in Ti–10V–2Fe–3Al alloy under isothermal forging condition. In: Blenkinsop PA, Evans WJ, Flower HM, editors. Titanium 95, science and technology. London: Institute of Materials; 1996. p. 1272–80.
[17] Welsch G. Technical note 1: metallography and microstructure. In: Boyer RR, Welsch G, Collings EW, editors. Materials properties handbook: titanium alloys. Materials Park (Ohio), ASM International; 1994. p. 1051–60.
[18] Chen CC, Hall JA, Boyer RR. High strength beta titanium alloy forgings for aircraft structural applications. In: Kimura H, Izumi O, editors. Titanium 80: science and technology. Japan: Kyoto; May 1980. p. 457–66.
[19] Boyer RR, Kuhlman GW. Processing properties relationships of Ti–10V–2Fe–3Al. Met Trans 1987;18A(December):2095–103.
[20] Kubiaku K, Sieniawski J. Effect of forging conditions and annealing temperature on fatigue strength of two phase titanium alloys. Mater Des 1997;18(4/6):365–7.
[21] Ismarrubie ZN, Aidy Ali, Satake T, Sugano M. Influence of microstructures on fatigue damage mechanisms in Ti-15-3 alloy. Mater Des 2011;32:1456–61.
[22] Lutjering G, Williams JC. Titanium – engineering materials and processes. 2nd ed. Berlin: Springer Verlag; 2007.
[23] Bania PJ. Beta titanium alloys and their role in the titanium industry. In: Eylon D, Boyer RR, Koss DA, editors. Beta titanium alloys in the 1990's. Pennsylvania (Warrendale): TMS; 1993. p. 3–14.
[24] Bhattacharjee A, Joshi Vydehi A, Hussain SM, Gogia AK. Effect of thermomechanical processing on evolution of α phase morphology in β titanium alloys. In: Gorynin IV, Ushkov SS, editors. Titanium 99: science and technology, vol. I. St. Petersburg, CRISM, Prometey; 2000. p. 164–71.
[25] Margolin H, Cohen P. Evolution of the equiaxed morphology of phases in Ti–6Al–4V. In: Kimura H, Izumi O, editors. Titanium 80: science and technology. Kyoto: Japan; May 1980. p. 1555–61.
[26] Margolin H, Cohen P. Kinetics of evolution of alpha in Ti–6Al–4V. In: Kimura H, Izumi O, editors. Titanium 80: science and technology. Kyoto: Japan; May 1980. p. 2991–7.
[27] Hirth JP, Froes FH. Correlations between fracture toughness and other mechanical properties in titanium alloys. Met Trans 1977;8A:1165–77.

[28] Froes FH, Chestnut JC, Rhodes CG, Williams JC. Toughness and fracture behavior of titanium, ASTM STP 651, Philadelphia, PA: ASTM. p. 115–53.
[29] Ninomi M, Kobayashi T. Fracture characteristics analysis related to the microstructures in titanium alloys. Mater Sci Eng 1996;A 213:16–24.
[30] Eylon D, Seagle SR. State of Titanium in the USA – the first 50 years. In: Gorynin IV, Ushkov SS, editors. Titanium 99: science and technology, vol. I. St. Petersburg, CRISM, Prometey; 2000. p. 37–47.